Growth, thermal desorption and low dose ion bombardment damage of C_{60} films deposited on Cu(111)

Journal of Physics Communications

OPEN ACCESS

RECEIVED
22 June 2017

REVISED
22 September 2017

ACCEPTED FOR PUBLICATION
26 September 2017

PUBLISHED
8 November 2017

PAPER

Growth, thermal desorption and low dose ion bombardment damage of C_{60} films deposited on Cu(111)

F Bonetto[1,2], **R A Vidal**[1,3], **V Quintero Riascos**[1], **C J Bonin**[1,3] **and J Ferrón**[1,2]

[1] Instituto de Física del Litoral (CONICET-UNL), Güemes 3450, S3000GLN Santa Fe, Argentina
[2] Departamento de Materiales, Facultad de Ing. Química, Universidad Nacional del Litoral, Santiago del Estero 2829, S3000AOM Santa Fe, Argentina
[3] Departamento de Física, Facultad de Ing. Química, Universidad Nacional del Litoral, Santiago del Estero 2829, S3000AOM Santa Fe, Argentina

E-mail: bonetto@ifis.santafe-conicet.gov.ar

Keywords: film growth, thermal desorption, low dose irradiation damage, fullerenes

Abstract

Auger electron spectroscopy (AES), low energy electron diffraction (LEED) and reflection electron energy loss spectrometry (REELS) were used to characterize the growth and thermal stability of C_{60} films deposited on Cu(111). By means of LEED we found that while C_{60} grows in an ordered fashion up to the first monolayer (ML) at room temperature (RT), it turns amorphous beyond that point. On the other hand, when the substrate temperature is kept at 450 K, films up to two ML with crystalline structure are obtained. For substrate temperatures beyond 570 K thick films (more than 1 ML) do not grow at all. By using AES, we found that a thick C_{60} film starts to desorb at a temperature around 470 K but the first ML remains stable up to temperatures as high as 900 K. A ML with a better crystalline order is obtained after desorption than that growth with the substrate at RT or higher temperatures. When the substrate is heated at 970 K, the first ML is not fully removed but the C_{60} molecular structure is altered or molecules break up into smaller pieces. The ion induced damage on C_{60} on Cu(111) films was studied for typical ions, incoming energies and irradiation doses used in low energy ion scattering (LEIS) experiments. The *D*-value of C(KLL) Auger spectra, the π-plasmon of REELS and the evolution of the LEIS spectra, were monitored to characterize the damage caused to the film. We found that, at low doses ($\sim 10^{14}$ ions cm^{-2}), damage is only detectable for massive ions like Ar, but not for H and He in the 2–8 keV range.

1. Introduction

Fullerenes have been extensively studied since its discovery in 1985 [1]. Due to its applications in very diverse fields, like medicine, electronics, chemistry, etc [2], they have aroused the interest of the scientific community. Similarly, a large number of articles were dedicated to the fundamental properties of fullerenes, some of them focused on the growth of C_{60} films on different substrates [3–8]. In particular, the growth of C_{60} on semiconductor surfaces has been broadly investigated due to its applications in solar cell-based devices [9–12].

The literature on C_{60} films growth on metal substrates is abundant [8, 13–24]. Particularly on Cu(111) substrates, STM experiments combined with theoretical calculations of bands structure [16], and photoemission [19] were used to demonstrate that electron transfer from the Cu(111) substrate to C_{60} varies between 1 and 2 electrons per molecule. Sakurai *et al* [18], using field-ion STM (technique that combines an STM with field emission microscopy), show substantial differences in the C_{60} growth on Cu (111) and Ag (111), mainly due to the strong C_{60}–Cu (111) interaction. Later, LEED [20] and STM [22] studies show that C_{60} adsorption of molecules on a Cu(111) surface induces a reconstruction of the substrate, and a recent Auger study [8] shows that C_{60} films on Cu(111) grow layer by layer (LbL).

Alternatively, only a few articles were devoted to the study of thermal desorption of fullerene films deposited on different substrates, e.g. polymers [25, 26]; alumina, silicon, graphite and carbon nanotubes [13, 27–29]; and some metal substrates like Ta, Ag, Au and Al [15, 30].

On the other hand, techniques based on the dispersion of slow ions (low energy ion scattering, LEIS) are widely used for chemical and structural surface characterization [31]. The technique has a high surface sensitivity, being possible to detect fractions of monolayer (ML) using low doses with minimal radiation damage. In particular, this is important for certain carbonaceous nanostructured surfaces, wherein the irradiation damage can be important for certain irradiation conditions. Recently [32], it has been shown that the technique is capable of checking the purity of graphene surfaces, demonstrating the benefits of the technique in screening the quality of the graphene during its fabrication process.

Despite damage on C_{60} films under ion bombardment having been previously studied, most of these works were focused on high incoming energies (>20 keV), high irradiation doses or different incoming projectiles [33–42]. The modification of fullerene films using ion beams in the LEIS regime (ion energy <10 keV) has barely been studied [43–47]; focusing mostly on Ar^+ incoming projectiles. Among these articles, it is relevant to mention that a direct knock-out of a single carbon atom from C_{60} molecules have been observed for high impact energies (>13.5 keV) of Ar^{2+} and He^{2+} collisions on C_{60} molecular clusters, leading this process to an efficient formation of new systems like C_{58}^+, C_{59}^+, C_{118}^+ and C_{119}^+ [42, 48].

In the present work we studied the growth and thermal stability of C_{60} films on Cu(111) as an extension of a previous research were we studied the growth of C_{60} on Cu(111) with AES and kinetic Monte Carlo simulations [8]. We use Auger electron spectroscopy (AES), for elemental composition information; reflection electron energy loss spectrometry (REELS), for molecular structural information; and low energy electron diffraction (LEED), for crystalline structural information. With these techniques, we are able to determine the effect of surface temperature on molecular stability and accommodation. On the other hand, we assess the optimal irradiation conditions (ion type, dose, and incoming energy) under which LEIS experiments can be carried on with minimum damage of C_{60} films deposited on Cu (111).

2. Experimental methods

Thick C_{60} films were deposited by vacuum sublimation of C_{60} powder (at 625 K) on a Cu(111) single crystal. The sample was positioned at a distance of 5 cm right in front of the Knudsen cell containing the C_{60} powder. The whole process was carried out under ultra-high vacuum (UHV) conditions ($\sim 10^{-9}$ Torr).

Desorption measurements have been performed by using a commercial Auger spectrometer (SAM PHI 590 A) based on a UHV chamber and equipped with a cylindrical analyzer and a coaxial electron gun. The experimental setup and the sample preparation procedure were described in a previous paper [8].

The following procedure was used to study the C_{60} films thermal desorption. Starting from a thick C_{60} film deposited on Cu(111), the C(KLL) and Cu(MVV and LVV) Auger spectra were monitored as the sample temperature was increasing from room temperature (RT) (300 K) to about 1000 K. The sample was heated by electron rear bombardment and the temperature measured by a chromel-alumel thermocouple. Auger spectra were acquired in differential mode (modulation: 4 V_{p-p}), by using a 3 keV (1 μA) electron beam. Alternatively, REELS spectra of the sample were taken in order to analyze the π-plasmon peak dependence with sample temperature. In this case, the electron incident energy was fixed to 100 eV.

Irradiation damage and LEED experiments were performed in a different UHV chamber equipped with a LEIS-TOF spectrometer, and a LEED/Auger system. Briefly, this system consists of: (i) a UHV chamber with a base pressure of 10^{-9} Torr ; (ii) an ion gun (Colutron), equipped with a Wien filter, beam focusing lenses and beam pulsing plates; (iii) a time-of-flight (TOF) spectrometer; and (iv) a LEED/AES system based on a 4 mesh reverse view retractable optics and a coaxial miniature electron gun (VG model RVL 900).

Before C_{60} evaporation, the substrate was carefully cleaned via several cycles of sputtering (6 keV Ar^+, 30° incident angle) and annealing (850 K, 5 min). The sample cleanness was checked by Auger measurements of the level of typical contaminants (carbon and oxygen).

Once the substrate was prepared, a thick C_{60} film was evaporated as above described. The thickness of the C_{60} film was controlled through the evaporation time. The deposition rate was estimated by LEED measurements for coverages under the first ML. The differences in the growth rate, produced by the change in the sticking coefficient, in going from C_{60} on Cu(111) to C_{60} on C_{60}, has been already shown to be negligible [8].

In order to assess if typical LEIS experiments can be performed on this sample, i.e., to check the sample damage under typical irradiation doses in LEIS experiments; the sample was exposed to irradiation with various ions and range of incident energies (both usual in LEIS experiments). Ar^+, He^+ and H^+ were used as projectiles with energies of 2, 4 and 8 keV, and an incident angle of 22.5° (respect to the surface). The irradiation time was fixed to 8 h of a pulsed ion beam (average current density: 15 nA cm^{-2}). To monitor the irradiation damage on

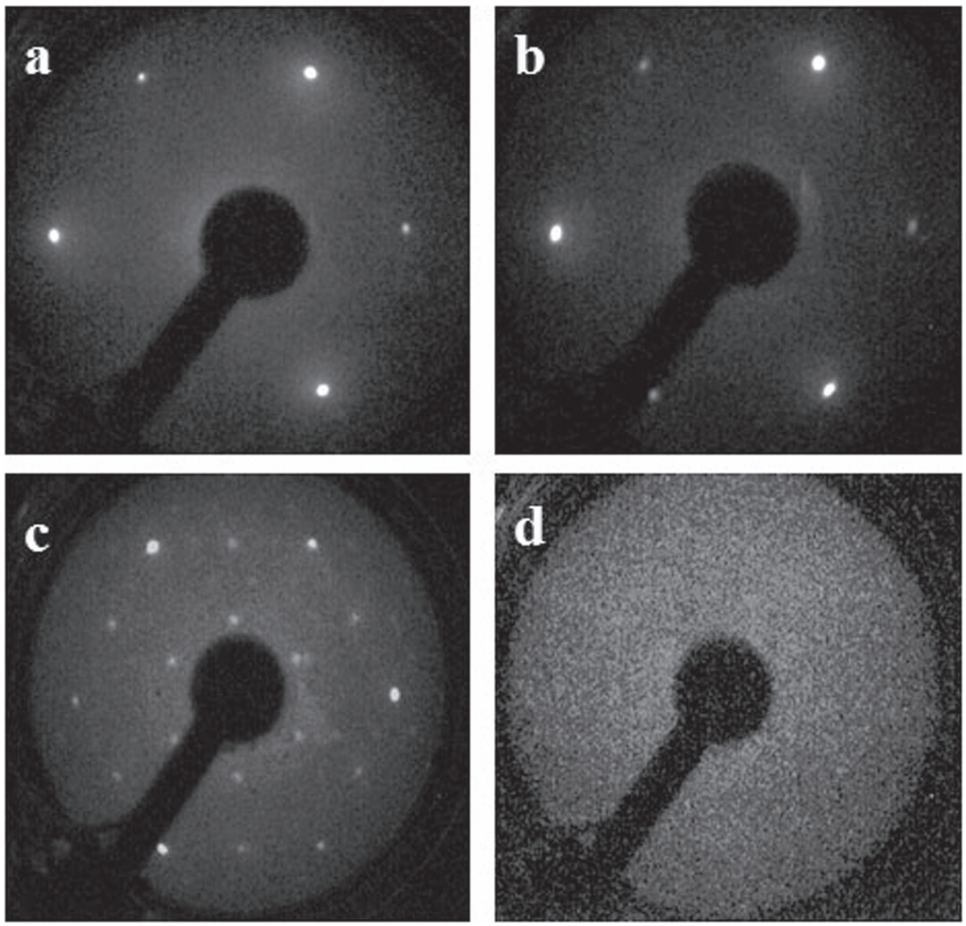

Figure 1. LEED images taken with a 100 eV electrons primary energy. (a) Clean Cu(111) surface, just before starting C_{60} evaporation, (b) after 10 min of C_{60} deposition, (c) after 25 min of C_{60} evaporation, and (d) after 50 min. The substrate temperature was kept at $T = 293$ K during the whole experiment.

C_{60} films, REELS spectra (100 eV primary energy) and AES (3 keV primary energy) were taken before C_{60} deposition, immediately after C_{60} evaporation, in regular 2 h time intervals during pulsed irradiation; and after continuous irradiation ($\sim 1\ \mu A\ cm^{-2}$).

LEIS-TOF spectra were acquired for 3 keV Ar^+, 6 keV He^+ and 5 keV H^+ irradiation at a scattering angle of 45°. For Ar^+ irradiation, three spectra (15 min acquisition time each) were sequentially acquired. For He^+ and H^+ irradiation, several spectra were consecutively taken (6 min each), compared and summed over time in order to gain information on time evolution and enhance the signal to noise ratio.

3. Results and discussion

3.1. C_{60} growth on Cu(111). LEED results

The different growing stages of C_{60} on Cu(111) were monitored via LEED images taken with 100 eV primary energy electrons at a fixed substrate temperature of 293 K (RT). In figure 1 we show the LEED images that describe the growth process, starting from a clean copper surface to a thin C_{60} film.

The clean Cu surface is characterized by LEED immediately before starting the C_{60} evaporation (figure 1(a)), showing the typical hexagonal Cu(111) LEED pattern. After 10 min of evaporation, corresponding to 0.4 ML according to the AES calibration, a more blurred spot pattern, consistent with the formation of an incomplete ML of C_{60} molecules (figure 1(b)), is obtained. After 25 min of evaporation, a clear change in the original LEED pattern is observed (figure 1(c)). The symmetry (4×4) of the pattern reveals the formation of a commensurate ML of C_{60} on the Cu(111) substrate [22, 49], showing the LbL growth, at least up to the first ML in agreement with previous measurements using AES [8]. Increasing the film thickness, (50 min of evaporation) produces the loss of the LEED pattern (figure 1(d)), indicating that the ordered structure is not preserved beyond the formation of the first layer. This result is also consistent with the formation of an amorphous-like C_{60} film on the Cu(111) substrate.

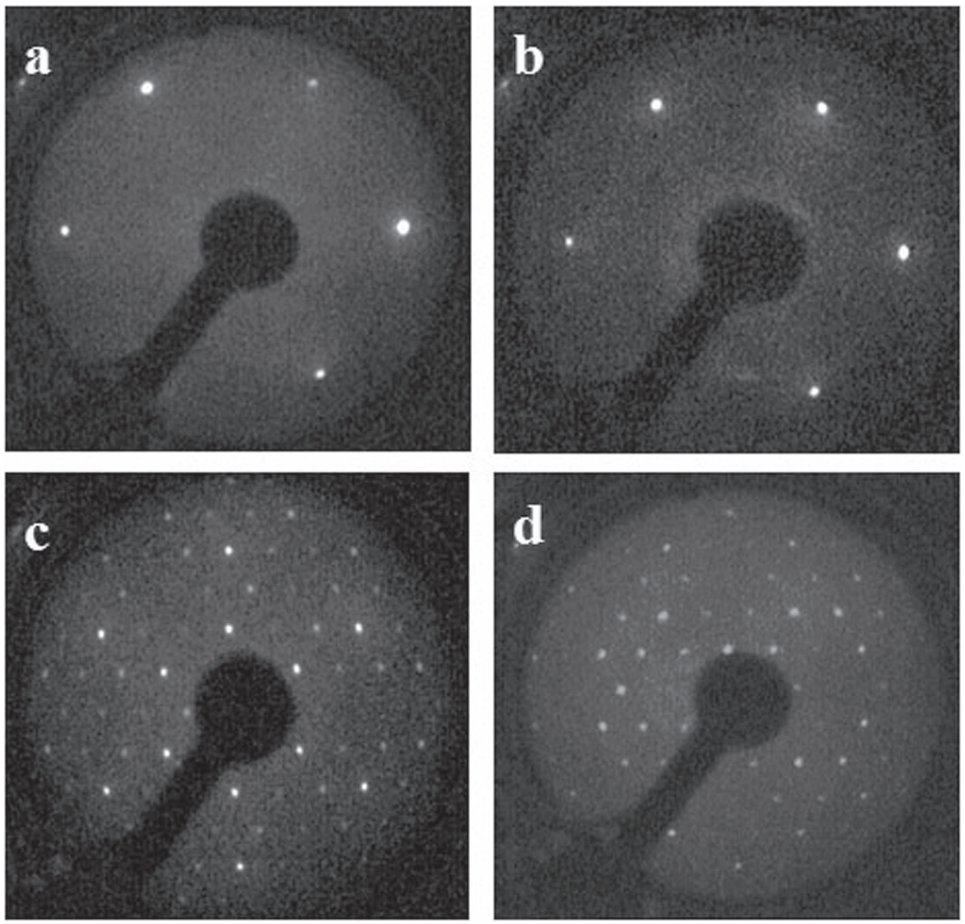

Figure 2. LEED image for C_{60} evaporated on Cu(111) when the substrate temperature is kept at 570 K for clean Cu(111) (a); after 10 min of C_{60} deposition (b); after 25 min (c); and after 50 min (d).

We have already shown that C_{60} grows in a LbL fashion at RT up to three MLs [8] and that only one ML grows if the substrate is kept at a high temperature (570 K). However, we did not find any differences on how the first layer grows under both situations. This is not a surprising result since AES is not sensitive to the size of the growing island. LEED offers the possibility of gaining information in this sense. In figure 2 we show evolution of the grow of C_{60} on Cu(111) at 570 K.

While the first three adsorption stages (images 2(a)–(c)) essentially reproduce the RT experiment, the LEED image corresponding to the fourth adsorption stage (evaporation time: 50 min) completely changed (figure 2). The pattern shown in figure 2(d) is similar to the one shown in figures 1(c) and 2(c) but with the diffraction spots more clearly defined, which confirms that when the substrate temperature is greater than 570 K only one ML grows on the copper surface. The higher definition of the LEED spots can be associated to the larger domains with crystalline order when the C_{60} film is grown with the substrate kept at 570K.

We also explore the possibility of growing a thicker C_{60} film with a long-range crystalline structure by heating the substrate at temperatures lower than 570 K. In this test, the substrate was kept at 470 K while C_{60} was evaporated for the same deposition times as in figure 1. The corresponding LEED images obtained are shown in figure 3. The pattern obtained in figure 3(d) is clearly different from that shown in figure 1(d). Now the diffraction spots can be easily recognized, showing that the thick film deposited presents crystalline structure. The high substrate temperature is probably inducing a rapid rearrangement of the C_{60} molecules leading to a long-range crystalline order.

3.2. Thermal desorption of C_{60} films on Cu(111)

Figure 4 shows the evolution of the Auger peak to peak heights of C (KLL) and Cu (MVV and LVV) while the temperature of the sample is increased from RT (300 K) to 973 K. The experiment started with a thick C_{60} film (~3 ML) deposited on the Cu(111) surface. The temperature dependence of the ratios C/Cu(MVV) and C/Cu (LVV) are shown in the inset of figure 4.

The amplitudes of the Auger signal do not significantly change until the substrate temperature reaches ~470 K, indicating the absence of any significant C_{60} desorption in this temperature range. From that

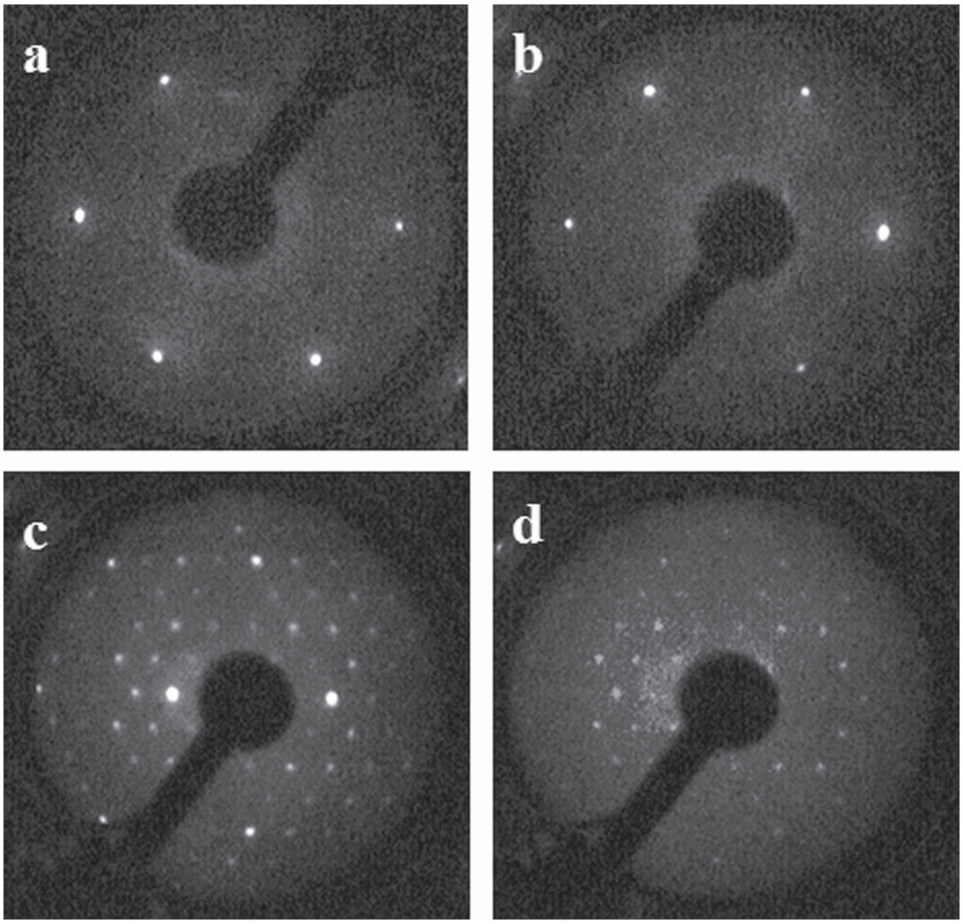

Figure 3. LEED image for C_{60} evaporated on Cu(111)at 450 K: (a) clean Cu(111) surface, before C_{60} evaporation, (b) after 10 min of C_{60} deposition, (c) after 25 min, and (d) after 50 min. The pattern is different from that observed in figure 1(d), indicating a crystalline structure formation.

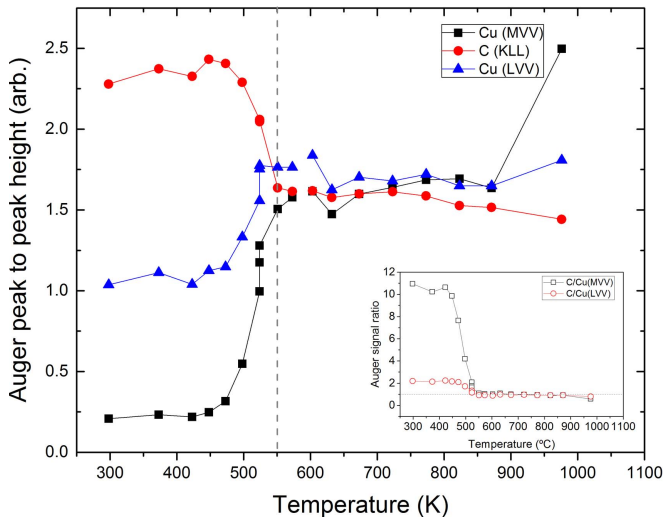

Figure 4. Auger peak to peak height for C (KLL) and Cu (MVV and LVV), for different substrate temperatures. The vertical dashed line ($T \sim 550$ K) denotes the temperature from which only one monolayer of C_{60} is still remaining on the Cu(111) substrate. The ratios C/Cu(MVV) and C/Cu(LVV) are shown in the inset. The whole desorption process takes place at temperatures between 450 K and 550 K.

temperature on, until ca. 550 K, the C(KLL)/Cu Auger signal ratios start to decrease consistent with a C_{60} desorption process. From 550 to 900 K, the C and Cu Auger signals remain constant, pointing out the absence of any kind of carbon desorption. This finding is probably linked to the stability of only one ML in this ample temperature range (550–900 K).

For temperatures higher than 900 K the Cu Auger signal ratios starts increasing while the C signal shows only a slight decrease, suggesting that the C_{60} molecules are kept adsorbed on the Cu(111) surface, but undergoing some changes in their molecular structure (e.g. breaking of molecular bonds). A similar behavior was found by Hamza *et al* [28] when C_{60} molecules are desorbed from Si(100) at 900 K. They showed that C_{60} molecules might start breaking into fragments that covers a large fraction of the silicon surface.

In order to gain information about this C_{60}/Cu(111) thermal desorption process, LEED images were taken. The starting point was a thick film (~3 ML) of C_{60} deposited on Cu(111). In figure 5 we show the images taken at increasing temperatures: 290 (a); 450 (b); 570 (c); (d) 770; and 970 K (e).

Different remarks can be made based on previous images: (i) the crystalline structure (order) starts to recover at temperatures close to 450 K; (ii) the typical LEED pattern of one C_{60} ML on Cu(111) becomes sharper when the temperature is increased ((c) and (d)), (iii) while the C_{60} crystalline order is lost at temperatures around 900 K, the LEED pattern of clean Cu(111) (figure 1(a)) is never recovered. From these findings, we can infer that: (i) the C_{60} ML attached to the Cu(111) atoms (first ML) is not thermally desorbed (even at $T = 970$ K); (ii) up to temperatures of 450 K, the LEED pattern (figure 5(b)) is consistent with long-range crystalline order, indicating a reordering of C_{60} molecules; (iii) second and upper layers are thermally desorbed between 450 and 770 K and, (iv) according to AES and LEED results C_{60} molecules could break up into smaller fragments that might spread all over the substrate; explaining the important C/Cu Auger ratio and the absence of crystalline structure revealed by LEED.

In order to assess potential changes in the C_{60} molecules structure, reflected electron energy loss spectra were taken during thermal desorption process. The π-plasmon, due to π-bonds of C_{60} molecule, was monitored during the process (figure 6).

Three distinctive features can be recognized in the REELS spectra when the temperature is increased: (i) the π-plasmon gets broader mostly in the first stages of the C_{60} thermal desorption; (ii) a slight shift (~0.8 eV) of the π-plasmon to a higher energy loss is observed when temperature rises from 670 to 1070 K indicating changes in the C_{60} molecular structure and (iii) the clean Cu(111) spectrum is, even at the highest temperatures, never retrieved. The latter result is fully consistent with previous Auger and LEED observations.

3.3. Ion bombardment damage under low irradiation doses

With the purpose of determining whether it is possible to analyze C_{60} thin films grown on Cu with LEIS, we performed a systematic study aimed to assess the potential irradiation damages produced with typical ions, irradiation doses and incoming energies used in LEIS experiments. The study essentially consisted on irradiating the sample during a fixed period of time (8 h) with a pulsed ion current (typical of LEIS-TOF experiments). Auger and REELS spectra were taken every 2 h to monitor sample damage during the experiment. After the 8 h of pulsed ion-current irradiation, the sample was directly irradiated (non-pulsed current) during 10 min. The study was performed for different incoming energies (2, 4 and 8 keV) and various projectile ions (H^+, He^+ y Ar^+).

The bar charts plotted in figure 7 show the ratio of C(KLL)/Cu(MVV) Auger peak to peak signal for four different stages of the study: (i) clean Cu (black); (ii) thick C_{60} film deposited on Cu(111) just before irradiation (red); (iii) after 8 h of pulsed irradiation (green) and (iv) after 10 min of direct irradiation (blue). Results are shown for H^+ (figure 7(a)), He^+ (figure 7(b)) and Ar^+ (figure 7(c)) for 3 different incoming energies: 2, 4 and 8 keV (indicated).

Similarly, in figure 8 REELS spectra are shown for the same experimental conditions as in figure 7. In these figures, the region corresponding to the π-plasmon is zoomed in.

As it can be clearly observed from figures 7 and 8, the comparison between the spectra obtained at different stages of the study, both techniques provide the same apparent result: changes are only detected (within the experimental error) when the sample was irradiated with Ar^+, regardless of the incoming ion energy.

An additional damage test was performed by using the *D* parameter of the C(KLL) peak [50–52] in order to determine whether the sp^3/sp^2 content was modified under ion irradiation. According to [50], the distance between the maximum and minimum value of the KLL carbon peak is linked to the sp^3/sp^2 C-bonding type ratio. In this way, compounds with molecular structure close to graphite (100% sp^2 bonds) have a *D* parameter close to 21 eV and compounds structurally close to diamond (100% sp^3 bonds) present a *D* parameter of the order of 13 eV. Analogously, amorphous carbon or carbon black pellets (what is expected when C_{60} molecule is destroyed) present a *D* parameter closer to diamond. In figure 9 we show a comparison of C KLL spectra taken at different irradiation stages. The C_{60} pristine film spectrum (red) is taken as a reference. For it, the *D* parameter is

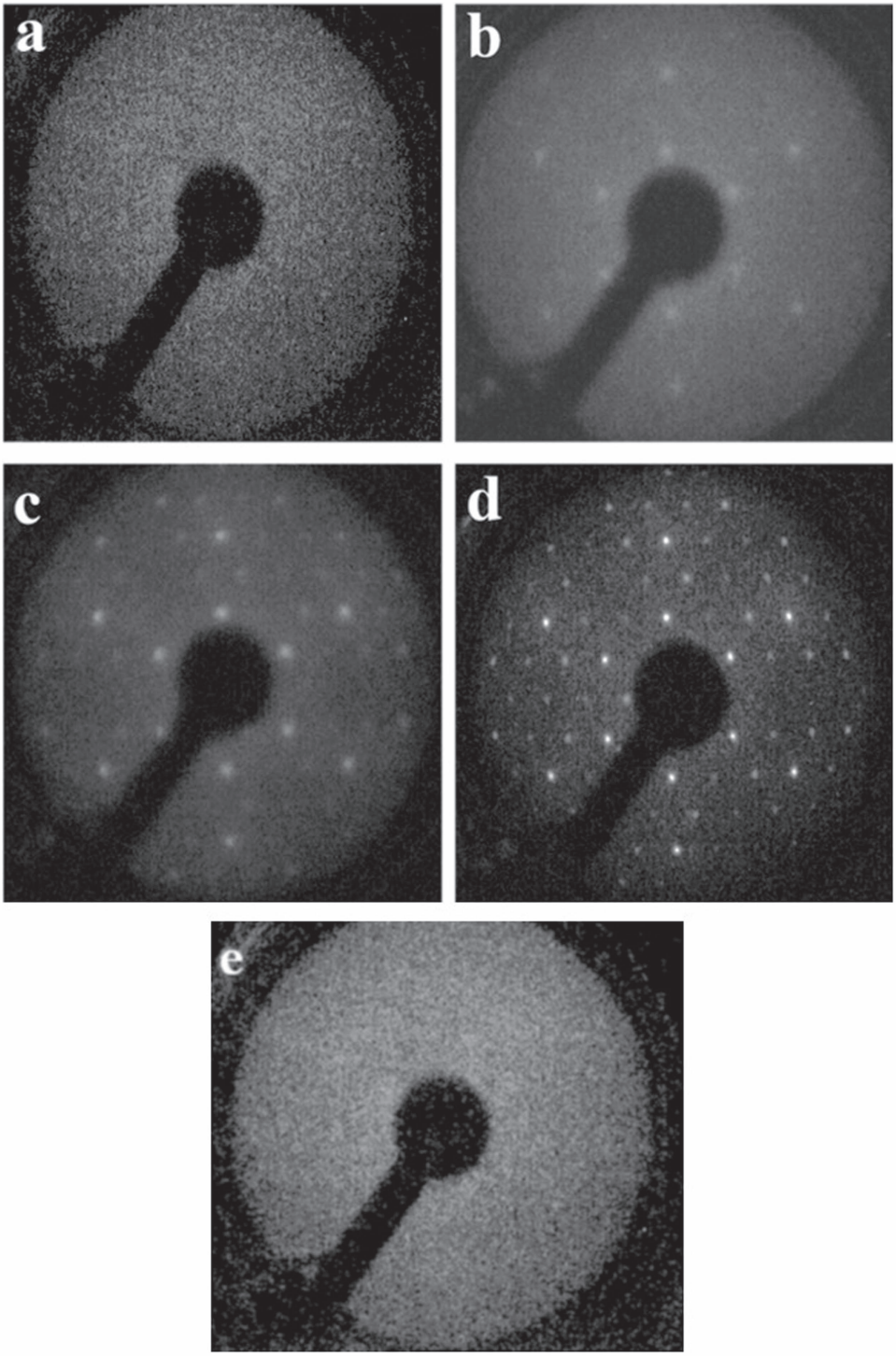

Figure 5. Thermal desorption process of a C_{60} film deposited on Cu(111) studied by LEED: (a) LEED image of a thick C_{60} film on Cu(111) at room temperature; (b) after heating the substrate at 450, (c) at 570, (d) at 770 and (e)970 K. The sample temperature was kept constant during 5 min before each image was taken.

of the order of 23 eV indicating a molecular structure with almost 100% of sp^2 hybridization. From the figure it is clear that the *D* parameter of the films irradiated with H^+ and He^+ does not change even at high incoming energies. However, if Ar^+ is used as the projectile, the Auger peak structure is strongly modified and the *D* parameter cannot be straightforwardly obtained anymore. This issue is a clear sign of destruction at molecular level.

To check if knockout processes of single carbon atoms were prompted during irradiation, we perform a LEIS-TOF study. In LEIS, recoil carbon atoms generated during the collision, can be easily detected if the scattering angle is not too large. In figure 10 we show LEIS spectra for 3 keV Ar^+, 6 keV He^+ and 5 kev H^+ ions colliding with a thick film of C_{60} deposited on Cu(111) taken with a fixed scattering angle of 45°.

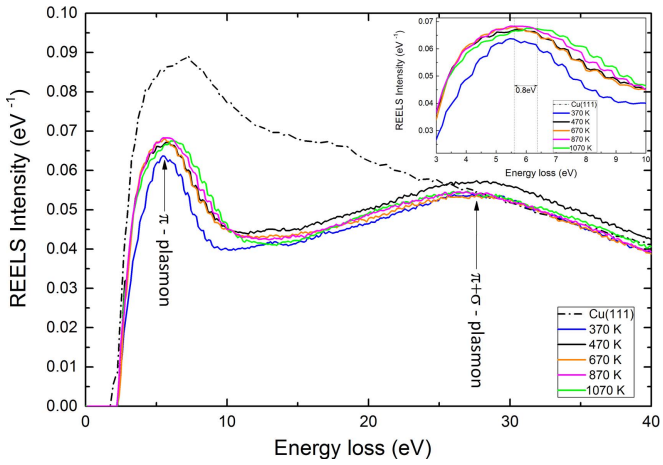

Figure 6. Reflected energy loss spectra (REELS) for different substrate temperatures. The π-plasmon (inset) is broaden and shifted during the thermal desorption process. The clean Cu spectrum is never recovered, consistent with previous Auger and LEED results.

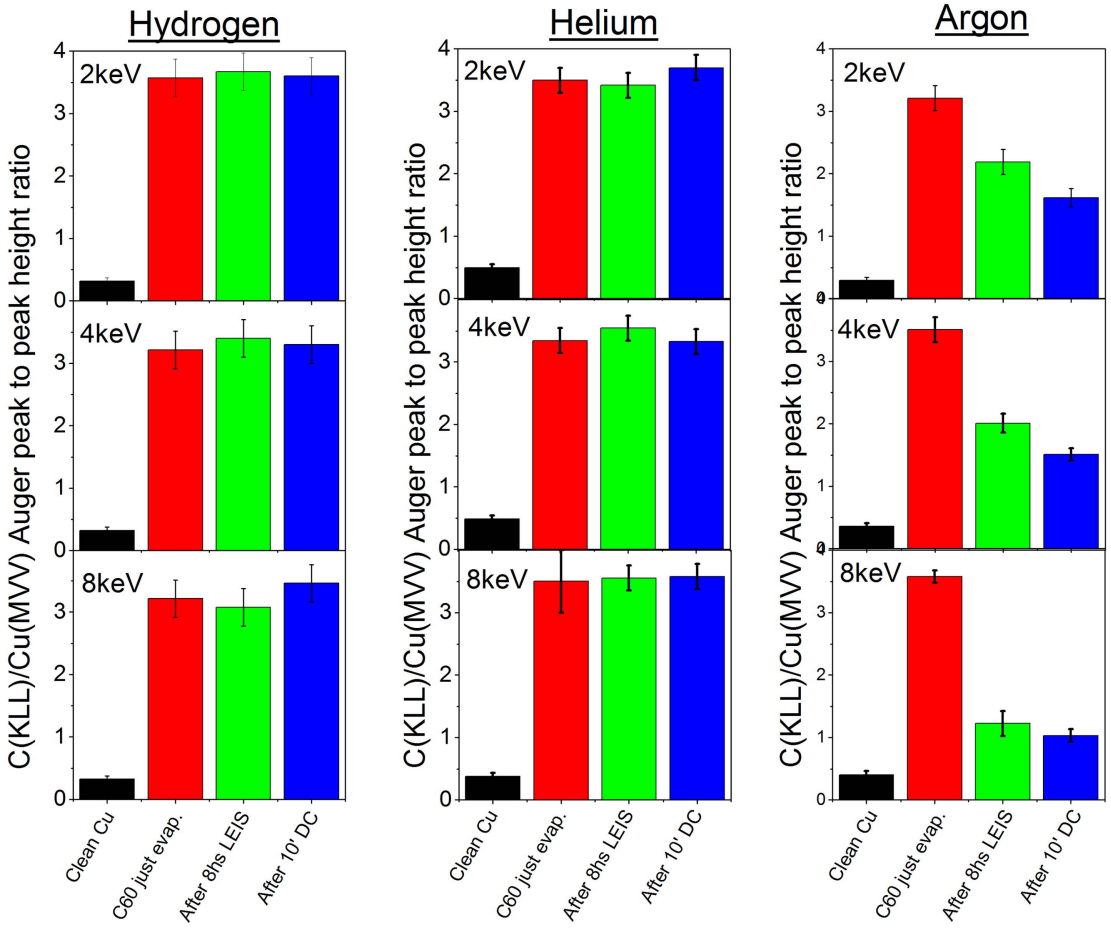

Figure 7. C(KLL)/Cu(MVV) Auger peak to peak height ratio for the different situations of the experiment: before C_{60} evaporation or clean Cu (black); just after C_{60} deposition (red), after 8 h of pulsed irradiation (green), and after 10 min of direct irradiation (blue). The corresponding incoming energies are indicated. Only appreciable differences are observed when projectile Ar^+ ions are used.

For 3 kev Ar^+ irradiation, three successive spectra were taken, each with 15 min acquisition time. In the first spectrum (black) only the peak corresponding to C atom recoils is seen, showing that knockout processes are taking place during the irradiation.

For the subsequent spectra (red and green) the peak due to the elastic scattering of Ar^+ ions from copper atoms is also appreciated, indicating that an important fraction of the C_{60} molecules were removed, and the

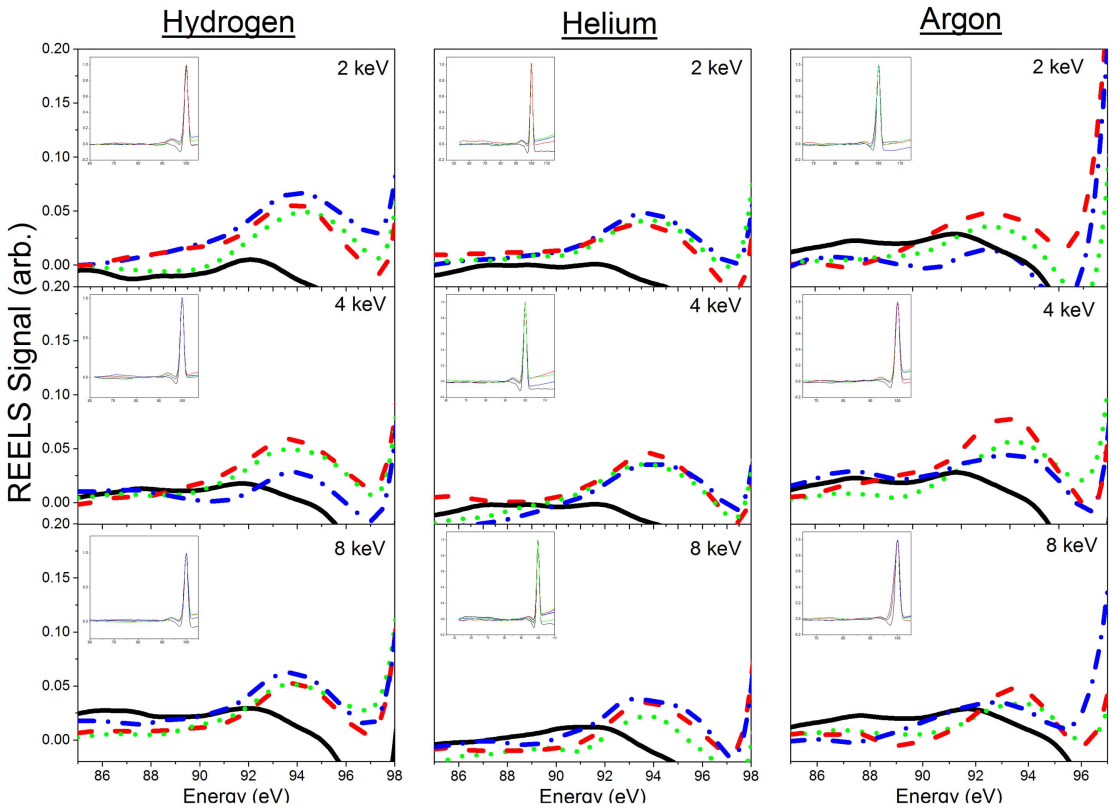

Figure 8. Reflected energy loss spectra of the sample under H^+ (left), He^+ (middle) and Ar^+ (right) irradiation taken after 8 h of pulsed irradiation (green) and after 10 min of direct irradiation (blue). Both are compared with the control situation: after C_{60} deposition (no irradiation) (red) and, clean Cu (black). The incoming energies of the projectile ions are indicated. Again, signals of damage are observed only under Ar irradiation.

projectile already interacts with substrate atoms (Cu). This peak increases with time due to the steady sputtering of C_{60} molecules. The clean Cu(111) spectrum (gray) is shown for comparison.

For 6 kev He^+ irradiation (center), and 5 kev H^+ irradiation (right) the LEIS spectra is shown for 2 h acquisition time. Both spectra show the unique presence of the direct elastic peak due to the scattering of the projectiles with the C atoms of the C_{60} molecule. The total absence of the C recoil peak clearly indicates that knockout processes of single carbon atoms are not taking place under these irradiation conditions.

4. Conclusions

LEED results show that the first C_{60} ML adsorbed on the Cu(111) surface presents long range crystalline order that disappears as the C_{60} subsequent layers are formed. It is also revealed by LEED that when the temperature of the substrate is kept at about 600 K during the C_{60} deposition, only one ML grows on Cu(111). When the C_{60} is evaporated under desorption temperatures like 450 K, the second C_{60} layer grows with crystalline order. Rapid molecular reordering induced by the sample temperature might be responsible for this behavior.

Starting from a thick, amorphous like C_{60} film (3 ML or more), the molecules start to desorb at temperatures ca. 470 K, remaining only one ML at temperatures higher than 570 K. Auger, LEED and REELS measurements show that even at 800 K the first C_{60} ML does not desorb. However, results obtained by the three techniques at temperature higher than 950 K, indicate that even when some form of carbon always remains, the C_{60} molecules are structurally modified (possible breaking).

No damage was detected when the sample was irradiated with H^+ or He^+ with doses and irradiation times usual in LEIS experiments under pulsed irradiation conditions (fluence below 3×10^{14} ions cm^{-2}), or direct irradiation (4×10^{15} iones cm^{-2}). On the other hand, Auger, REELS and LEIS spectra revealed that the C_{60} is damaged (altered) when the sample is irradiated with Ar^+, even when using low projectiles incoming energies (2 keV) and low pulsed irradiation doses. Four independent methods (REELS spectra, Auger peak to peak ratio, Auger C(KLL) *D*-factor and LEIS spectra) consistently lead to previous conclusion. Our Ar irradiation results agree with previous work done on ion beam modification of fullerene films by 2 keV Ar ions [43]. They studied the induced amorphization of fullerene films using EELS and determined a cross section for the destruction of

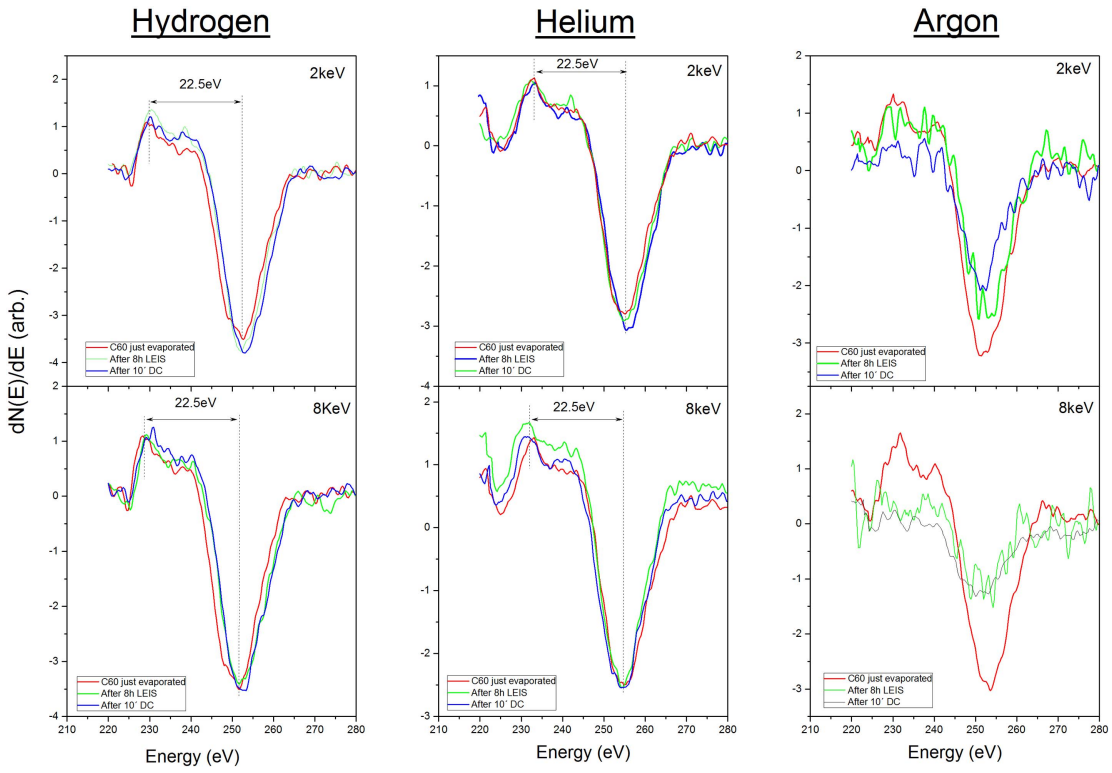

Figure 9. Comparison of C(KLL) Auger spectra for the different situations analyzed (for the sake of simplicity, the 4 keV incoming energy case is omitted). The distance in energy between the maximum and the minimum of the spectrum (*D*-factor) is not modified when H^+ and He^+ are used as incoming ions. When Ar^+ is used as a projectile, the spectra is strongly modified and the distance cannot be straightforwardly obtained.

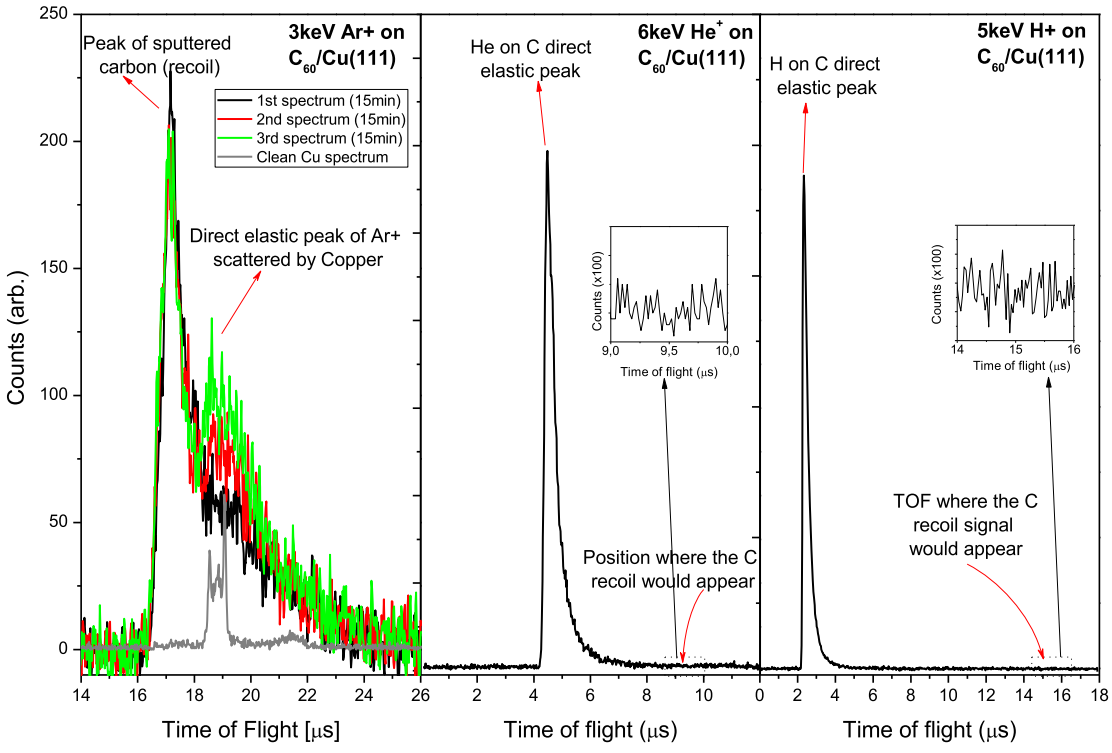

Figure 10. LEIS-TOF spectra for 3 keV Ar + ions (left), 6 keV He + ions (center) and 5 keV H + ions (right) colliding with a thick C_{60} film deposited on Cu(111). A clear sample modification is perceived during Ar^+ irradiation. No signs of single C atoms knockout processes during He^+ and H^+ irradiation are observed (no peaks are observed in inset graphs).

the C_{60} molecules of 8.5×10^{-15} cm^2, value that corresponds closely to the geometric size of one C_{60} molecule, and suggesting that each incident Ar ion destroys one molecule upon ion impact. Our result of no damage of C_{60} for low energy He^+–C_{60} collisions are in line with a previous gas-phase study [47] where small clusters of Polyclinic Aromatic Hydrocarbon and C_{60} molecules are fragmented in 9 keV collisions with Ne, but not with He.

Our results are also consistent with sputtering coefficients calculated via SRIM code [53] (www.srim.org). For an ion beam with 4 keV incident energy impinging at 22.5° from the surface (geometry used in the present experimental setup) the following sputtering coefficients are obtained: 0.01, 0.06 and 0.86 for H^+, He^+ and Ar^+, respectively. Another relevant parameter also in line with our results is the deposition of nuclear energy (S_n, nuclear stopping power). For instance, the nuclear stopping power of 4 keV Ar^+ incident ions is 30 times higher than the corresponding one of He^+ and almost 300 times higher than H^+ nuclear stopping power. Regarding the role of the electronic energy deposition, the value of the electronic stopping power (S_e) does not change as much as the nuclear stopping power. For example for 4 keV ions $S_e = 11.3$, 6.6 and 6.2 eV Å^{-1}, for Ar^+, He^+ and H^+, respectively. Although for light ions (H^+ and He^+) S_e is much greater than S_n the deposition of electronic energy does not seem to be an important factor in the irradiation damage of C_{60} thin films.

From these results, it is possible to conclude that H^+ and He^+ are suitable to be used as projectiles in LEIS analysis whereas Ar^+ projectiles are inappropriate to study C_{60} films.

Acknowledgments

Economic support from CONICET (grant PIP 2012–2014 No. 0577), ANPCyT (grant PICT 2010 No. 0294 and PICT 2013 No. 0164) and UNL (grant CAI + D 2011 No. 501 201101 00283 LI) is acknowledged.

ORCID iDs

F Bonetto https://orcid.org/0000-0001-8596-7971

References

[1] Kroto H W, Heath J R, O'Brien S C, Curl R F and Smalley R E 1985 C_{60}: buckminsterfullerene *Nature* **318** 162–3
[2] Amelines-Sarria O *et al* 2011 Electronic and magnetic properties of C_{60} thin films under ambient conditions: a multitechnique study *Org. Electron.* **12** 1483–92
[3] Fleming R M *et al* 1991 Preparation and structure of the alkali-metal fulleride A_4C_{60} *Nature* **352** 701–3
[4] Xu H, Chen D M and Creager W N 1993 Double domain solid C_{60} on Si(111)-7 × 7 *Phys. Rev. Lett.* **70** 1850–3
[5] Radeva E, Georgiev V, Spassov L, Koprinarov N and Kanev S 1997 Humidity adsorptive properties of thin fullerene layers studied by means of quartz micro-balance *Sensors Actuators* B **42** 11–3
[6] Pascual J I, Gómez-Herrero J, Rogero C, Baró A M, Sánchez-Portal D, Artacho E, Ordejón P and Soler J M 2000 Seeing molecular orbitals *Chem. Phys. Lett.* **321** 78–82
[7] Liu H and Reinke P 2006 C_{60} thin film growth on graphite: coexistence of spherical and fractal-dendritic islands *J. Chem. Phys.* **124** 164707
[8] Vidal R A and Ferrón J 2015 A detailed Auger electron spectroscopy study of the first stages of the growth of C_{60} thin films *J. Phys. D: Appl. Phys.* **48** 435302
[9] Datta D and Kumar S 2009 Growth and ellipsometric studies on C_{60} thin films for solar cell applications *J. Appl. Phys.* **106** 074517
[10] Brabec C J, Gowrisanker S, Halls J J M, Laird D, Jia S and Williams S P 2010 Polymer–fullerene bulk-heterojunction solar cells *Adv. Mater.* **22** 3839–56
[11] Bastos J P, Voroshazi E, Fron E, Brammertz G, Vangerven T, Van der Auweraer M, Poortmans J and Cheyns D 2016 Oxygen-induced degradation in C_{60}-based organic solar cells: relation between film properties and device performance *ACS Appl. Mater. Interfaces* **8** 9798–805
[12] McAfee T, Apperson A, Ade H and Dougherty D B 2016 Growth of thermally stable crystalline C_{60} films on flat-lying copper phthalocyanine *J. Mater. Chem.* A **4** 1028–32
[13] Tokmakoff A, Haynes D R and George S M 1991 Desorption kinetics of C_{60} multilayers from Al_2O_3 (0001) *Chem. Phys. Lett.* **186** 450–5
[14] Chase S J, Bacsa W S, Mitch M G, Pilione L J and Lannin J S 1992 Surface-enhanced Raman scattering and photoemission of C_{60} on noble-metal surfaces *Phys. Rev.* B **46** 7873–7
[15] Altman E I and Colton R J 1993 The interaction of C_{60} with noble metal surfaces *Surf. Sci.* **295** 13–33
[16] Hashizume T *et al* 1993 Intramolecular structures of C_{60} molecules adsorbed on the Cu(111)-(1 × 1) surface *Phys. Rev. Lett.* **71** 2959–62
[17] Hunt M R C, Modesti S, Rudolf P and Palmer R E 1995 Charge transfer and structure in C_{60} adsorption on metal surfaces *Phys. Rev.* B **51** 10039–47
[18] Sakurai T, Wang X D, Hashizume T, Yurov V, Shinohara H and Pickering H W 1995 Adsorption of fullerenes on Cu(111) and Ag(111) surfaces *Appl. Surf. Sci.* **87–88** 405–13
[19] Tsuei K-D, Yuh J-Y, Tzeng C-T, Chu R-Y, Chung S-C and Tsang K-L 1997 Photoemission and photoabsorption study of C_{60} adsorption on Cu(111) surfaces *Phys. Rev.* B **56** 15412–20
[20] Pai W W, Hsu C-L, Lin M C, Lin K C and Tang T B 2004 Structural relaxation of adlayers in the presence of adsorbate-induced reconstruction: C_{60}/Cu(111) *Phys. Rev.* B **69** 125405

[21] Shi X-Q, Van Hove M A and Zhang R-Q 2012 Survey of structural and electronic properties of C_{60} on close-packed metal surfaces *J. Mater. Sci.* **47** 7341–55
[22] Xu G, Shi X-Q, Zhang R Q, Pai W W, Jeng H T and Van Hove M A 2012 Detailed low-energy electron diffraction analysis of the (4 × 4) surface structure of C_{60} on Cu(111): seven-atom-vacancy reconstruction *Phys. Rev.* B **86** 075419
[23] Matz D L, Ratcliff E L, Meyer J, Kahn A and Pemberton J E 2013 Deciphering the metal-C_{60} interface in optoelectronic devices: evidence for C_{60} reduction by vapor deposited Al *ACS Appl. Mater. Interfaces* **5** 6001–8
[24] Khosroabadi A A, Matz D L, Gangopadhyay P, Pemberton J E and Norwood R A 2014 Study of the C_{60}/Ag interface of a large area nanoarchitectured Ag substrate using surface-enhanced raman scattering *J. Phys. Chem.* C **118** 18027–34
[25] Pozdnyakov A O, Ginzburg B M, Maricheva T A, Kudryavtsev V V and Pozdnyakov O F 2004 Thermally stimulated desorption of C_{60} and C_{70} fullerenes from rigid-chain polyimide films *Physi. Solid State* **46** 1371–5
[26] Pozdnyakov A O 2006 Thermal desorption of fullerene C_{60} from polymer matrices *Compos. Sci. Technol.* **66** 3138–43
[27] Ulbricht H, Moos G and Hertel T 2003 Interaction of C_{60} with carbon nanotubes and graphite *Phys. Rev. Lett.* **90** 095501
[28] Hamza A V and Balooch M 1993 The chemisorption of C_{60} on Si(100)-(2 × 1) *Chem. Phys. Lett.* **201** 404–8
[29] Reinke P, Feldermann H and Oelhafen P 2003 C_{60} bonding to graphite and boron nitride surfaces *J. Chem. Phys.* **119** 12547–52
[30] Gall' N R, Rut'kov E V and Tontegode A Y 2005 Adsorption, desorption, and contact and thermal transformation of C_{60} molecules on a Ta(100) surface *Semiconductors* **39** 1280–4
[31] Brongersma H H, Draxler M, de Ridder M and Bauer P 2007 Surface composition analysis by low-energy ion scattering *Surf. Sci. Rep.* **62** 63–109
[32] Průša S *et al* 2015 Highly sensitive detection of surface and intercalated impurities in graphene by LEIS *Langmuir* **31** 9628–35
[33] Kastner J, Kuzmany H and Palmetshofer L 1994 Damage and polymerization by ion bombardment of C_{60} *Appl. Phys. Lett.* **65** 543–5
[34] Prawer S, Nugent K W, Biggs S, McCulloch D G, Leong W H, Hoffman A and Kalish R 1995 Ion-beam modification of fullerene *Phys. Rev.* B **52** 841–9
[35] Hunt M R C, Schmidt J and Palmer R E 1998 Electron-beam damage of C_{60} films on hydrogen-passivated Si(100) *Appl. Phys. Lett.* **72** 323–5
[36] Egerton R F and Takeuchi M 1999 Radiation damage to fullerite (C_{60}) in the transmission electron microscope *Appl. Phys. Lett.* **75** 1884–6
[37] Florian B 1999 Irradiation effects in carbon nanostructures *Rep. Prog. Phys.* **62** 1181
[38] Foerster C E, Serbena F C, Lepienski C M, Baptista D L and Zawislak F C 1999 The effect of fluence on the hardening of C_{60} films irradiated with He and N ions *Nucl. Instrum. Methods Phys. Res.* B **148** 634–8
[39] Zawislak F C, Baptista D L, Behar M, Fink D, Grande P L and da Jornada J A H 1999 Damage of ion irradiated C_{60} films *Nucl. Instrum. Methods Phys. Res.* B **149** 336–42
[40] Narumi K and Naramoto H 2002 Modification of C_{60} thin films by ion irradiation *Surf. Coat. Technol.* **158–159** 364–7
[41] Singhal R, Singh F, Tripathi A and Avasthi D K 2009 A comparative study of ion-induced damages in C_{60} and C_{70} fullerenes *Radiat. Eff. Defects Solids* **164** 38–48
[42] Zettergren H *et al* 2013 Formations of dumbbell C_{118} and C_{119} inside custers of C_{60} molecules by collision with alpha particles *Phys. Rev. Lett.* **110** 185501
[43] Hoffman A, Paterson P J K, Johnston S T and Prawer S 1996 Ion-beam-induced modification of fullerene films as studied by electron-energy-loss spectroscopy *Phys. Rev.* B **53** 1573–8
[44] Zhu Y, Yi T, Zheng B and Cao L 1999 The interaction of C_{60} fullerene and carbon nanotube with Ar ion beam *Appl. Surf. Sci.* **137** 83–90
[45] Reinke P and Oelhafen P 2002 Surface modification of C_{60} by ion irradiation studied with photoelectron spectroscopy *J. Chem. Phys.* **116** 9850–5
[46] Stockett M H *et al* 2014 Nonstatistical fragmentation of large molecules *Phys. Rev.* A **89** 032701
[47] Gatchell M *et al* 2014 Non-statistical fragmentation of PAHs and fullerenes in collisions with atoms *Int. J. Mass Spectrom.* **365** 260–5
[48] Seitz F *et al* 2013 Ions colliding with clusters of fullerenes—decay pathways and covalent bond formations *J. Chem. Phys.* **139** 034309
[49] Pai W W, Hsu C L, Lin K C, Sin L Y and Tang T B 2005 Characterization and control of molecular ordering on adsorbate-induced reconstructed surfaces *Appl. Surf. Sci.* **241** 194–8
[50] Mezzi A and Kaciulis S 2010 Surface investigation of carbon films: from diamond to graphite *Surf. Interface Anal.* **42** 1082–4
[51] Caschera D, Cossari P, Federici F, Kaciulis S, Mezzi A, Padeletti G and Trucchi D M 2011 Influence of PECVD parameters on the properties of diamond-like carbon films *Thin Solid Films* **519** 4087–91
[52] Kaciulis S 2012 Spectroscopy of carbon: from diamond to nitride films *Surf. Interface Anal.* **44** 1155–61
[53] Ziegler J F, Ziegler M D and Biersack J P 2010 SRIM—the stopping and range of ions in matter (2010) *Nucl. Instrum. Methods Phys. Res.* B **268** 1818–23